NASA CR-115852

ANALYSIS OF PLANETARY FLY-BY USING THE HELIOGYRO SOLAR SAILER

John M. Hedgepeth and Max D. Benton

ARC-R-296

August 9, 1968

ASTRO RESEARCH CORPORATION

SANTA BARBARA, CALIFORNIA

ANALYSIS OF PLANETARY FLY-BY USING THE HELIOGYRO SOLAR SAILER

John M. Hedgepeth and Max D. Benton

ARC-R-296

August 9, 1968

Prepared under Contract No. NAS7-427 by

ASTRO RESEARCH CORPORATION
Santa Barbara, California

for

NATIONAL AERONAUTICS AND SPACE ADMINISTRATION

SUMMARY

Mission analyses are made for the application of the Heliogyro solar-sailer concept to planetary fly-by with particular emphasis on Jupiter. The analysis takes into account the relationship between payload mass fraction and vehicle lightness number, performance characteristics for two launch vehicles, and the elementary planar equations of motion. Flight times are determined and optimized for various assumed sail-lightness numbers and for the two launch vehicles. Results show that 400 kg of (non-sail) payload can be placed in the vicinity of Jupiter in 470 days with a Titan IIIC-Burner II launch vehicle if a reasonable extension in polymer-film-fabrication state of the art is assumed. The same solar sailing mission can be done in 800 days with an Atlas SLV3C-Centaur launch vehicle.

INTRODUCTION

The use of solar pressure to provide propulsion for interplanetary space flight has been an attractive possibility for some time (Ref.1). Since "solar sailing" requires no expendable propellant the system has an infinite specific impulse and, therefore, is not time limited or velocity-increment limited. On the other hand, the available pressures are so low (0.9×10^{-5} newton per m^2 at 1 A.U. from the sun) that very large sail areas are required to produce reasonable forces.

One of the problems with the solar-sailing concept has been the difficulty of constructing the required large sail area. A concept has been recently created for doing this and for controlling the attitude of the sail with respect to the solar rays. This is the Heliogyro concept which makes use of centrifugal force to erect and rigidize the sails, and a combination of collective and cyclic pitch to produce the proper orientation. The mechanics of such a concept and some possible configurations are discussed in Reference 2. One of the simpler configurations is pictured in Figure 1. The sails are made of strips of aluminized polymer film which are stored on "window-shade" rollers and allowed to deploy as the vehicle is spun up. Changing of attitude is generated by pivoting the rollers to produce the proper pitch.

In Reference 2 some information is given as to the use of the Heliogyro in a manned flight to Mars and return. Recently considerable interest has arisen with regard to Jupiter fly-by missions. The purpose of this paper is to give the results of a study of the application of the Heliogyro to such a mission.

In this report, the various ingredients of the mission study are described and defined. Results are then obtained for the shortest flight times for given payloads and launch-vehicle configurations. The results are discussed, and directions for future work are recommended.

MISSION CONSIDERATIONS

The planetary fly-by mission considered consists of two phases: launch and interplanetary flight. The main attention herein is devoted to the second phase. The launch phase is considered only to the extent necessary to establish initial conditions for subsequent flight, which is assumed to be governed by simple two-body heliocentric orbital mechanics and to take place in the ecliptic plane.

Equations of Motion - Let U be the distance from the sun in astronomical units (A.U.), and ψ be the central angle traveled in radians. Also let the unit of time be the average time for the earth to travel a central angle of one radian and the unit of force to be the solar gravitational attraction on the spacecraft. Then the two-body equations can be written

$$U_{\tau\tau} - U\psi_{\tau}^{2} = \frac{D-1}{U^{2}} \tag{1}$$

$$U\psi_{\tau\tau} + 2U_{\tau}\psi_{\tau} = \frac{L}{U^{2}} \tag{2}$$

where D is the "drag" force on the sail (the component away from the sun) and L is the "lift" force (the component perpendicular to the vehicle-sun line). See Figure 2(a). Subscript notation has been used for derivatives.

Forces - The source of the lift and drag force is the solar pressure which is created by the reflection of photons from the sail. For a perfect reflector at one A.U. oriented perpendicular to the solar radiation the pressure is denoted by P_o. The actual pressures on a solar sail are different from this pressure because of orientation and reflectivity effects. The latter effect is small inasmuch as aluminized polymer films exhibit high specular reflectivities even after long simulated space exposure; it will therefore be ignored. The effect of orientation is to decrease the pressure as the cosine squared. An element of area dA, whose normal is oriented with respect to the solar radiation by angles θ in the ecliptic and φ out of the ecliptic (see Fig. 2(b)), will produce elemental lift and drag forces.

$$dL = \frac{\lambda}{A}\, dA \cdot \cos^3\varphi \cos^2\theta \sin\theta \tag{3}$$

$$dD = \frac{\lambda}{A}\, dA \cdot \cos^3\varphi \cos^3\theta \tag{4}$$

where λ , the so-called "lightness number", is

$$\lambda = \frac{P_o A}{[F]_{U=1}}$$

in which $F_{U=1}$ is the solar gravitational force at one A.U. Note that the lightness number is a force ratio which is independent of the distance to the sun since both forces follow the inverse-square law.

Clearly, for best performance, the intent should be to make $\varphi = 0$ and to maintain θ at its proper value over the entire sail. The local angles will vary somewhat from the ideal because of inability to control to the exact angle and because of unavoidable waviness of the centrifugally stiffened membraneous sail material. In an effort to obtain a quantitative idea of the influence of such variations on the performance, consider a situation wherein the local angles are statistical variables with an associated probability distribution function $f(\theta, \varphi)$. Thus, the probability that θ and φ lie in the intervals $\theta + d\theta$, and $\varphi + d\varphi$, respectively, is

$$f(\theta, \varphi)\, d\theta\, d\varphi$$

By making the usual assumptions about stationarity, ergodicity, and independence, all averages can be represented by the ensemble average. For example, for a general $G(\theta, \varphi)$,

$$G_{average} = \iint G(\theta, \varphi)\, f(\theta, \varphi)\, d\theta\, d\varphi \tag{5}$$

In the present case, then

$$L = \lambda \iint \cos^3\varphi \cos^2\theta \sin\theta\, f(\theta, \varphi)\, d\theta\, d\varphi \tag{6}$$

$$D = \lambda \iint \cos^3\varphi \cos^3\theta\, f(\theta, \varphi)\, d\theta\, d\varphi \tag{7}$$

Now, let the distribution be Gaussian, or

$$f(\theta,\ \varphi) = \exp[-(\theta-\theta_o)^2/2\sigma_\theta^2 - \varphi^2/2\sigma_\varphi^2] \tag{8}$$

In this assumption, θ_o can be viewed as the desired command angle, and σ_θ and σ_φ are the standard deviations from the desired value. Substituting into Eq. (5) and applying the method of steepest descent gives the following approximation

$$G_{average} = G(\theta_o,\ 0) + \frac{\sigma_\theta 2}{2} G_{\theta\theta}(\theta_o,\ 0) + \frac{\sigma_\varphi 2}{2} G_{\varphi\varphi}(\theta_o,\ 0)$$

In the present case this gives, for $\sigma_\theta = \sigma_\varphi = \sigma$

$$L = \lambda\cos^2\theta_o\ \sin\theta_o - \lambda\sigma^2\ \sin\theta_o\ (6\cos^2\theta_o-1) \tag{9}$$

$$D = \lambda\cos^3\theta_o - 3\lambda\sigma^2\ \cos\theta_o\ (2\cos^2\theta_o-1) \tag{10}$$

Note that the percentage decrement of lift exceeds that of drag; this will result in poorer performance as expected.

Payload Mass Fraction and Sail Lightness Number - The flight vehicle can be considered to be made up of the payload and the propulsion system. The payload consists of the basic structure, instruments, sensors, electronics, antennas, power supply, and so forth. The propulsion system consists of the sails, and all mechanisms necessary to deploy and control them, including the spinup rockets. The total vehicle mass can be written

$$M = M_p + M_s$$

where M_p is the payload mass and M_s is the mass of the propulsive (sail) system. Now, the payload mass fraction can be written as,

$$\frac{M_p}{M} = 1 - \frac{M_s}{M}$$

Since the lightness number is inversely proportional to mass, this can be rewritten

$$\frac{M_p}{M} = 1-\frac{\lambda}{\lambda_s} \tag{11}$$

where λ_s is the lightness number of the propulsive system. Call it the "sail lightness number".

The sail lightness number is a parameter of central importance to the present study. It assumes the same role for solar-pressure propulsion as does the specific impulse for reaction propulsion. A particular state of technology can be represented by a value of λ_s. Then tradeoffs between payload mass fraction and vehicle lightness number must be made in accordance with Eq. (11).

An idea of the attainable values of λ_s can be obtained from Figure 3 which shows the variation of lightness number, based on reflecting-membrane weight alone, with the polymer thickness for a polymer film clad with 3000 Å of aluminum. One-quarter mil polymer film is presently commercially available in large quantities, and laboratory samples of 0.05 mil film have been produced. Reasonable values of λ_s therefore range up to 0.5 for foreseeable technology growth. An upper limit of 5 has been derived (Ref. 3) for an all-aluminum film of sufficient thickness to avoid serious transparency. The studies herein will be limited to the range of $0.1 \leq \lambda_s \leq 0.5$.

Initial Conditions - At time $\tau = 0$, the vehicle is assumed to escape the earth's gravitational field, with an excess velocity of q at an angle β with the circle $U = 1$. Thus, at $\tau = 0$

$$U = 1 \tag{12}$$

$$U_\tau = q \sin\beta \tag{13}$$

$$\psi_\tau = 1 + q \cos\beta \tag{14}$$

The excess velocity q is, of course, produced by the launch vehicle and is a function of total spacecraft mass and, to a minor extent, of the launch trajectory. For the present purposes, the latter dependency can be ignored and the simple formula (in feet per second units)

$$q = \sqrt{V_c^2 - (36178)^2} \tag{15}$$

can be used. In this formula, V_C is the so-called characteristic velocity of the launch vehicle and is a function only of spacecraft mass.

Eq. (15) has been used in conjunction with launch-vehicle data to produce the curves of Figure 4 for the Titan IIIC/Burner II (1900) and the SLV3C/Centaur combinations. These curves will be used for the subsequent studies.

Programming of Sail Angle - The most difficult problem in minimizing the flight time is to control the sail angle in the proper fashion. This problem in trajectory optimization has been solved by Kelley (Ref. 4), but the methods are too complex to use herein. A near-optimum trajectory should be one in which power is maximized; that is, for which the sail is trimmed in such a way as to achieve the greatest energy input per unit time. Such a "maximum-power-trajectory" calculation has the simplifying advantage that the command sail angle is a function only of instantaneous flight parameters. Comparison with the results of Kelley indicates agreement within 2%, which is adequate for the present study.

The rate of energy input is

$$W_T = L\, U\psi_T + DU_T$$

$$= \lambda\cos^2\theta_o\,(U\psi_T\sin\theta_o + U_T\cos\theta_o)$$

where the error effects have been omitted since they would be difficult to take into account in a practical controller. Maximizing W_T yields

$$\tan\theta_o = -\frac{3}{4}\frac{U_T}{U\psi_T} + \sqrt{\frac{9}{16}\left(\frac{U_T}{U\psi_T}\right)^2 + \frac{1}{2}} \qquad (16)$$

RESULTS

The findings of the preceding section were used to calculate flight trajectories for a large number of configurations. The second-order Runge-Kutta method was employed with a time interval of 0.1 to integrate the equations of motion. Sample results are shown in Table I and Figure 5. The spacecraft reaches Mars ($U=1.52$ A.U.) in 83 days and Jupiter ($U=5.20$ A.U.) in 415 days. Sizeable radial velocities are developed (which, incidentally, may be undesirable because of short proximity times). The sail angle decreases rapidly from the maximum lift angle (35.3°) to around 20° and then decreases more gradually. The total thrust may be of interest in comparing with electric-propulsion results.

<u>Effect of Launch Angle</u> - The influence of β is shown in Figure 6. Here, times to Mars and Jupiter are plotted as a function of β for an excess velocity of 0.1 and two lightness numbers. The results show that although the optimum value of β is not zero (excess velocity is optimally inward for Jupiter flights and outward for Mars flights) the penalty of setting $\beta = 0$ is small. Therefore, this simplification has been made on all subsequent work.

<u>Effect of Random Errors</u> - The variation of flight time to Jupiter with magnitude of sail-angle error is shown in Figure 7. The increase in flight time is about 10% at a root-mean-square deviation of 8°. With suitable care, the rms deviation can probably be kept well under 5° and the effect would then be minor from the standpoint of preliminary mission studies. All subsequent results herein are based on the assumption that $\sigma = 0$.

<u>Basic Results</u> - As a result of the foregoing simplification the fly-by mission can be characterized by examining the flight time, which is a function only of launch excess velocity and vehicle lightness number. In Figure 8 curves are shown for the flight times to Mars and Jupiter versus excess velocity for several values of lightness number. The curves exhibit the expected trends, decreasing with either increasing λ or increasing excess velocity. Note that attractively short flight times are possible. Note also that the calculations were arbitrarily cut off after the first pass if insufficient radius was attained. The combination of these results with launch-vehicle capabilities and payload mass is discussed below.

Optimum Configuration - Consider a situation wherein a given payload mass is desired to fly near Jupiter with minimum transit time utilizing a given basic solar-sailing capability. In this case, M_p and λ_s are fixed, and the combination of M, q, and λ are sought that satisfies Eq. (11), utilizes Figure 4, and optimizes the flight time. By varying the lightness number λ, results such as those in Figure 9 can be obtained. The optimum can then be selected and plotted as in Figure 10.

In Figure 10 the available payloads are shown as a function of mission time for various sail lightness numbers. The results apply to the Jupiter fly-by mission utilizing either the Titan IIIC-Burner II or the Atlas SLV3C-Centaur launch vehicles. Clearly, the former launch vehicle yields much greater payloads, but is not nearly as advanced in actual development and, indeed, may not be available.

The curve for $\lambda_s = 0$ gives the purely ballistic capability of the Titan IIIC combination. Not only does the inclusion of solar sails with moderate λ_s appreciably increase the payload capability but also much more of the payload is useable inasmuch as no propellants are required for attitude control or mid-course guidance. The Heliogyro supplies those functions inherently.

The values of λ_s for the Atlas combination were selected to represent a reasonable reality of expectable sail technology in the near future. A value of $\lambda_s = 0.15$ can be obtained with presently available materials (slightly less than one-quarter mil film), and $\lambda_s = 0.3$ could be obtained if polymer film of one-tenth mil can be made available. Certainly, placing over 400 kg into the vicinity of Jupiter with an existing launch vehicle is an attractive possibility. Such a vehicle would have a total mass of 945 kg, a vehicle lightness number of 0.17 and a sail area of 0.1 square kilometers.

An interesting comparison exists between this latter solar sailer and a solar electric-propulsion vehicle recently proposed in Reference 5. For the same mission with the same launch vehicle, a payload weight of 290 kg is attained with a flight time of 900 days. The performance point on Figure 10 has been plotted to show the comparison.

CONCLUDING REMARKS

The study reported herein represents only a bare beginning toward a well-understood concept for Jupiter fly-by using the Heliogyro. It does, however, indicate that large gains in payload-delivery capability would occur and that further work should consequently be performed. One area of valuable endeavor would be to determine the effect on system parameters of putting terminal constraints on the mission. Another would be to investigate further the problem of sail-angle programming. The use of the gravity fields of other planets for producing major gains should also be examined, especially since the propulsive power of the Heliogyro becomes greater sunward and also could be used to correct the timing differences that otherwise make this technique only rarely possible.

In the system design area, many efforts are required to make the Heliogyro more than a paper concept. Theoretical analyses have been made; experiment is needed. Basic and developmental materials work is required to lower feasible film thickness to 0.05 mil and below.

REFERENCES

1. Garwin, "Solar Sailing, a Practical Method of Propulsion within the Solar System", Jet Propulsion, March 1958.

2. MacNeal, R.H., "The Heliogyro, an Interplanetary Flying Machine", Astro Research Corporation, ARC-R-249, March 13, 1967.

3. Cotter, T., "Solar Sailing", Sandia Corporation Research Coloquium SCR-78, April 1959, Office of Technical Services, Dept. of Commerce, Washington D.C.

4. Kelley, H.J., "Gradient Theory of Optimal Flight Paths", ARS Journal, Vol. 30, No. 10, pp. 947-954, October 1960.

5. Barber, T.A., Goldsmith, J.V., and Edberg, J.R., "Spacecraft Electric Propulsion - Now?", Astronautics & Aeronautics, Vol. 6, No. 6, June 1968.

TABLE I - SAMPLE FLIGHT TRAJECTORY

$\lambda = 0.26$
$q = 0.20$
$\beta = 0$
$\sigma = 0$

Time, Days	U, A.U.	ψ, Degrees	Velocity* Radial	Velocity* Circum.	θ, Degrees	Thrust**
.0	1.000	.000	.000	1.200	35.26	.1733
29.1	1.075	33.040	.297	1.161	28.39	.1740
58.1	1.282	58.923	.508	1.004	22.93	.1341
87.2	1.566	76.913	.611	.841	19.17	.0946
116.3	1.884	89.375	.654	.710	16.58	.0673
145.3	2.215	98.333	.668	.611	14.72	.0496
174.4	2.550	105.045	.670	.536	13.32	.0379
203.5	2.884	110.260	.665	.477	12.23	.0299
232.5	3.215	114.437	.658	.431	11.35	.0242
261.6	3.542	117.864	.650	.393	10.61	.0200
290.7	3.865	120.734	.642	.362	9.99	.0169
319.7	4.184	123.178	.634	.335	9.46	.0145
348.8	4.499	125.287	.626	.313	9.00	.0125
377.9	4.810	127.130	.618	.294	8.59	.0110
406.9	5.117	128.756	.611	.277	8.23	.0097
436.0	5.421	130.204	.605	.262	7.90	.0087
465.1	5.722	131.503	.599	.249	7.60	.0078
494.1	6.020	132.675	.593	.237	7.34	.0071
523.2	6.315	133.740	.587	.226	7.09	.0064
552.2	6.607	134.713	.582	.217	6.86	.0059
581.3	6.897	135.605	.577	.208	6.65	.0054
610.4	7.185	136.428	.573	.200	6.46	.0050
639.4	7.470	137.188	.568	.192	6.28	.0046
668.5	7.753	137.894	.564	.186	6.11	.0043
697.6	8.034	138.552	.561	.179	5.95	.0040
726.6	8.314	139.165	.557	.173	5.81	.0037
755.7	8.591	139.740	.553	.168	5.67	.0035
784.8	8.867	140.280	.550	.163	5.53	.0033
813.8	9.141	140.788	.547	.158	5.41	.0031
842.9	9.414	141.267	.544	.154	5.29	.0029
872.0	9.685	141.719	.541	.150	5.18	.0027
901.0	9.955	142.148	.538	.146	5.07	.0026

* Units of mean earth velocity around sun.
** Units of solar gravitation attraction at 1 A.U.

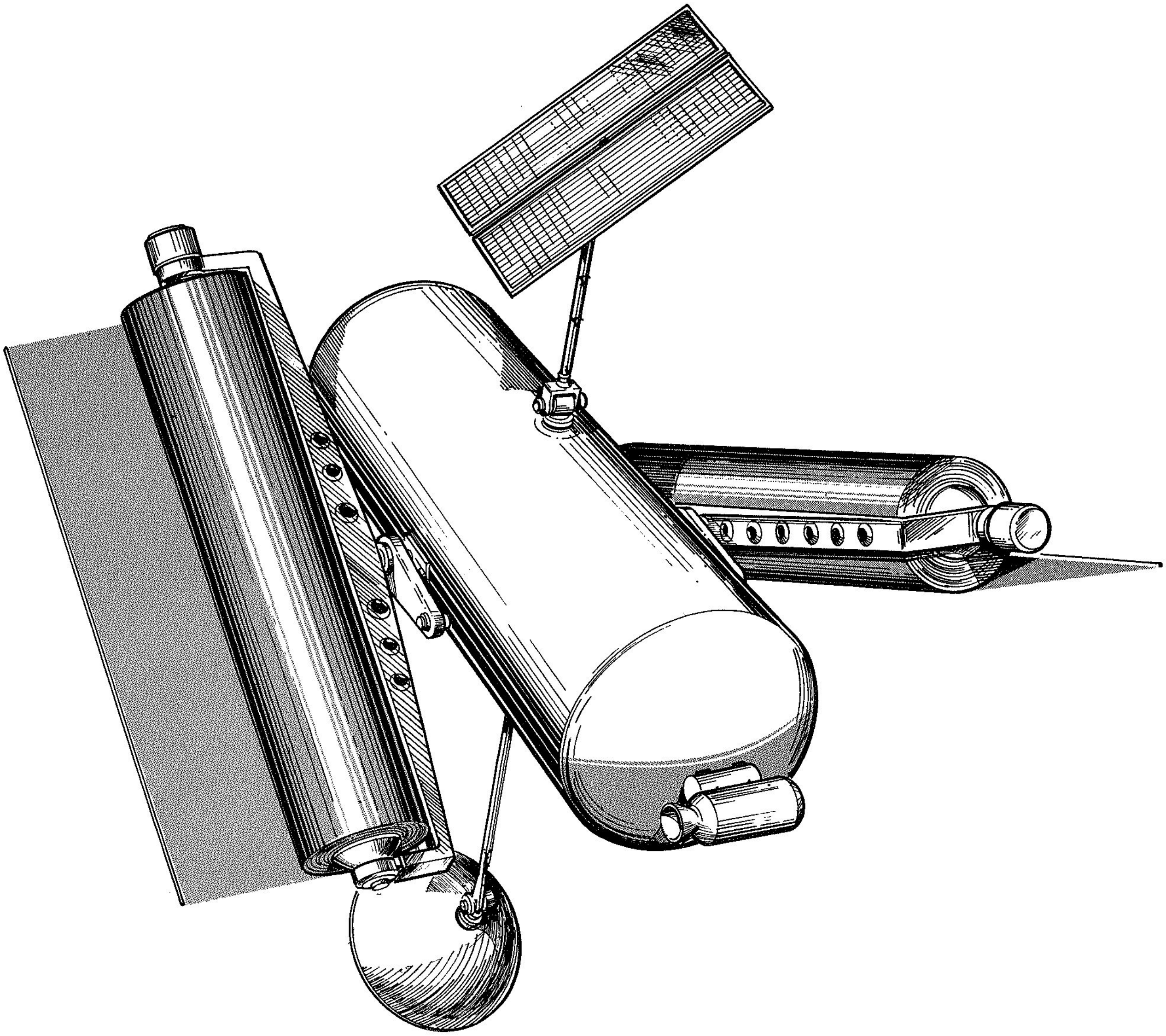

Figure 1. Sketch of Experimental Two-Blade Design

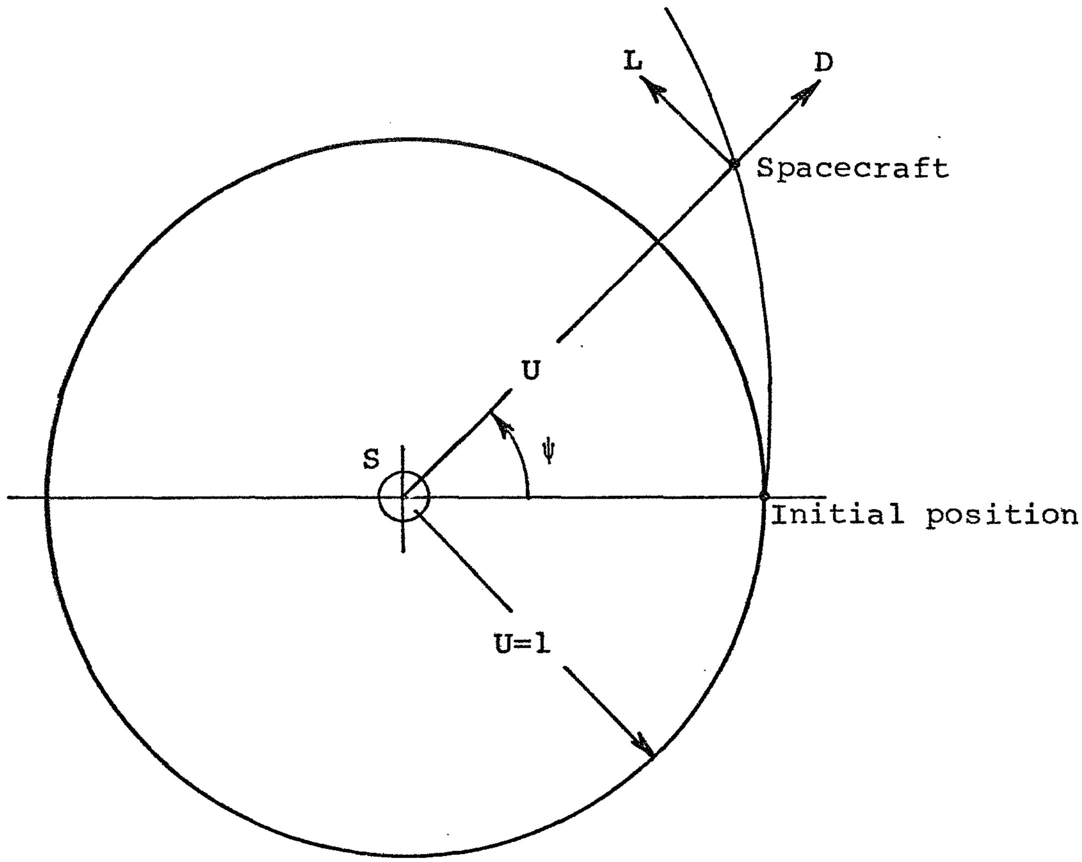

(a) Coordinates and forces

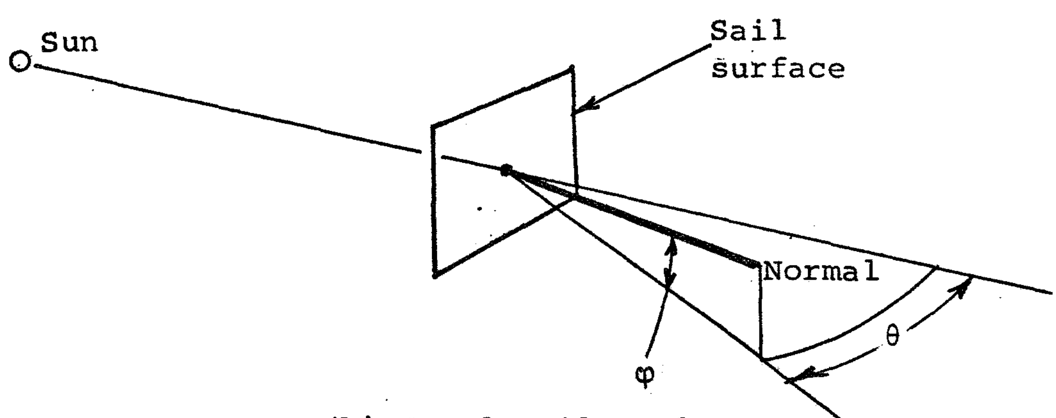

(b) Local sail angles

Figure 2. Geometry of Flight

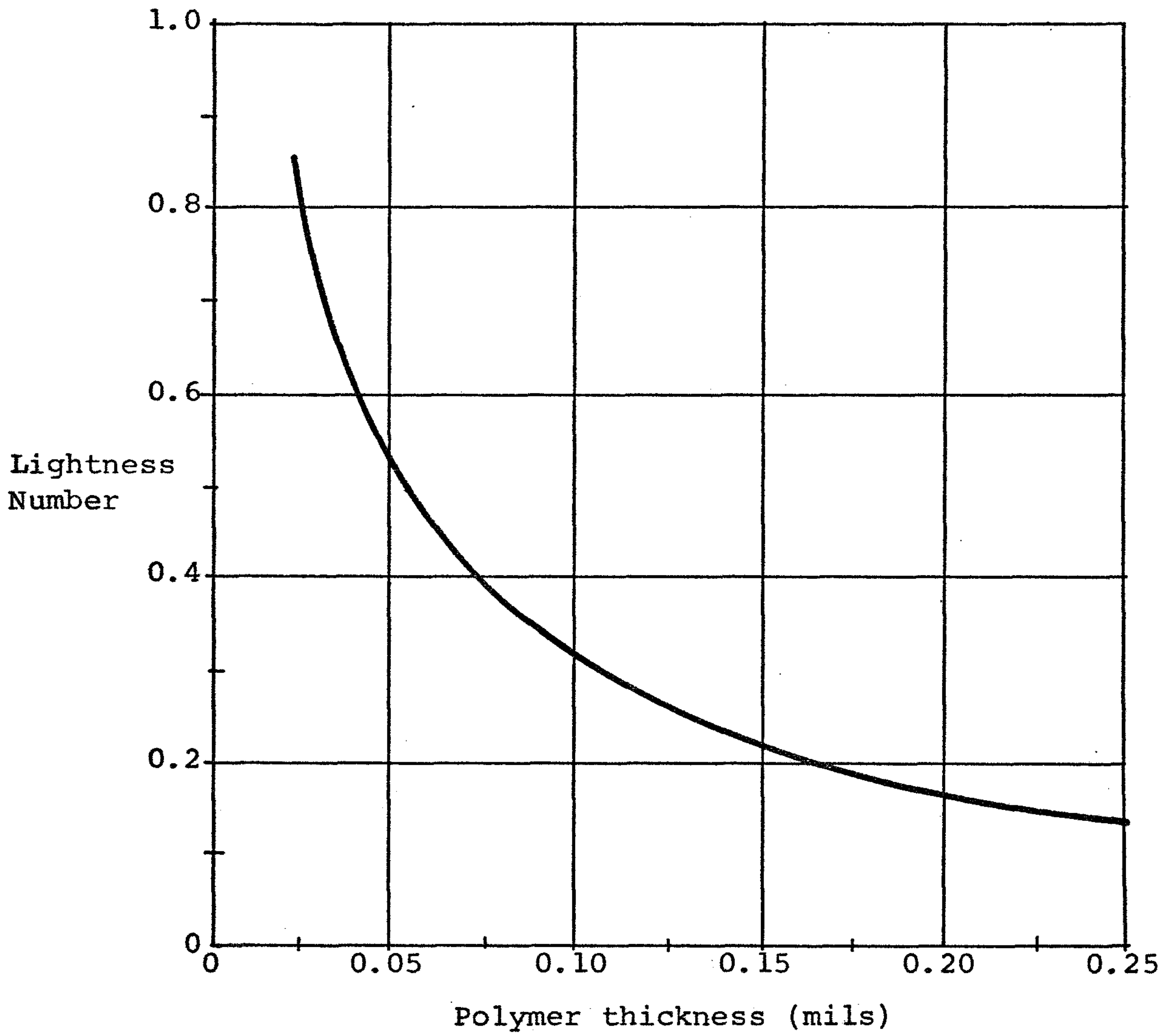

Figure 3. Film Lightness Number for Aluminized Polymer Sheet. (Polymer density 0.055 lb/cu in.; aluminum thickness 3000 Å)

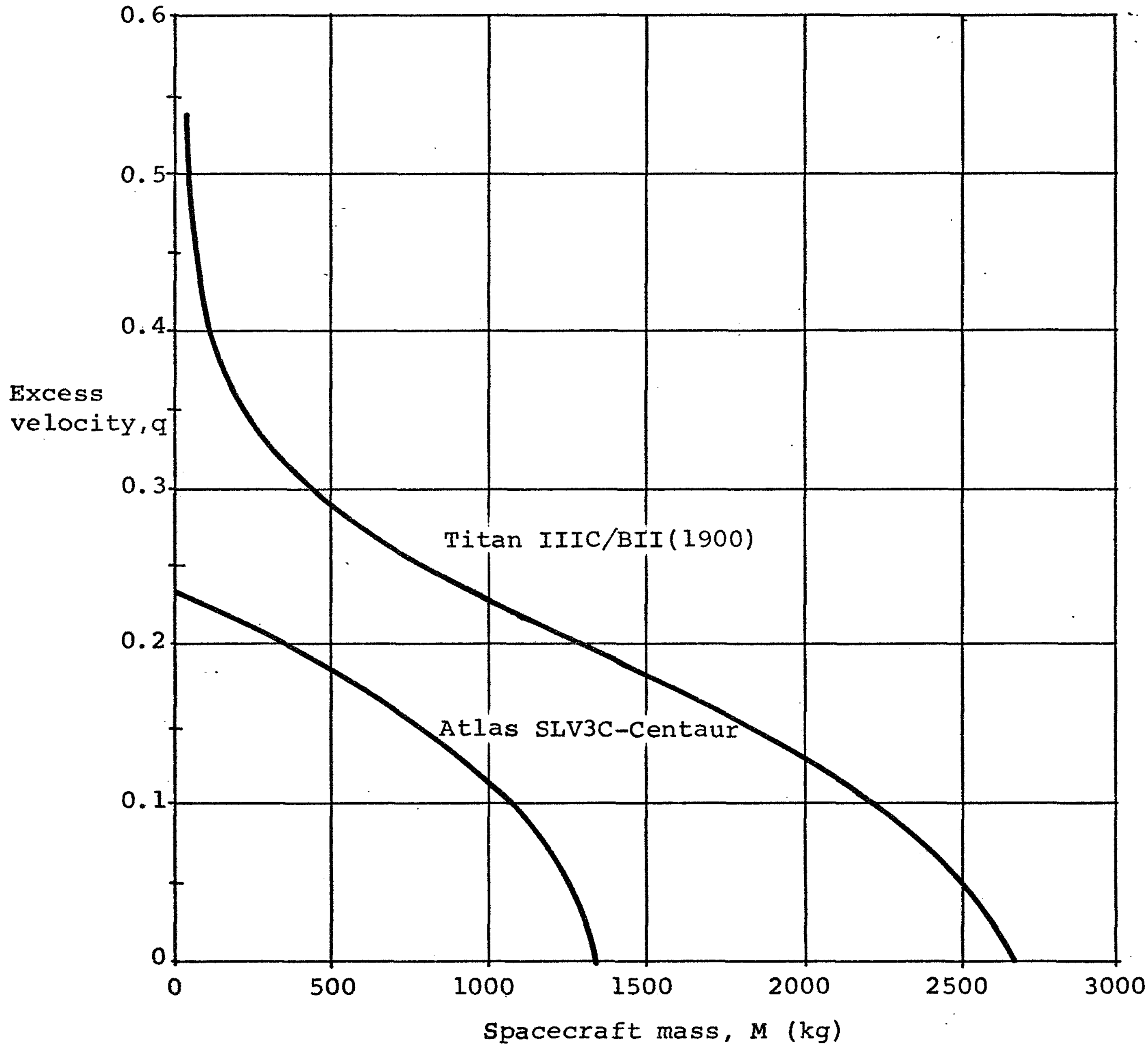

Figure 4. Variation in Excess Velocity with Payload Mass (Velocity measured in units of mean earth velocity around the sun)

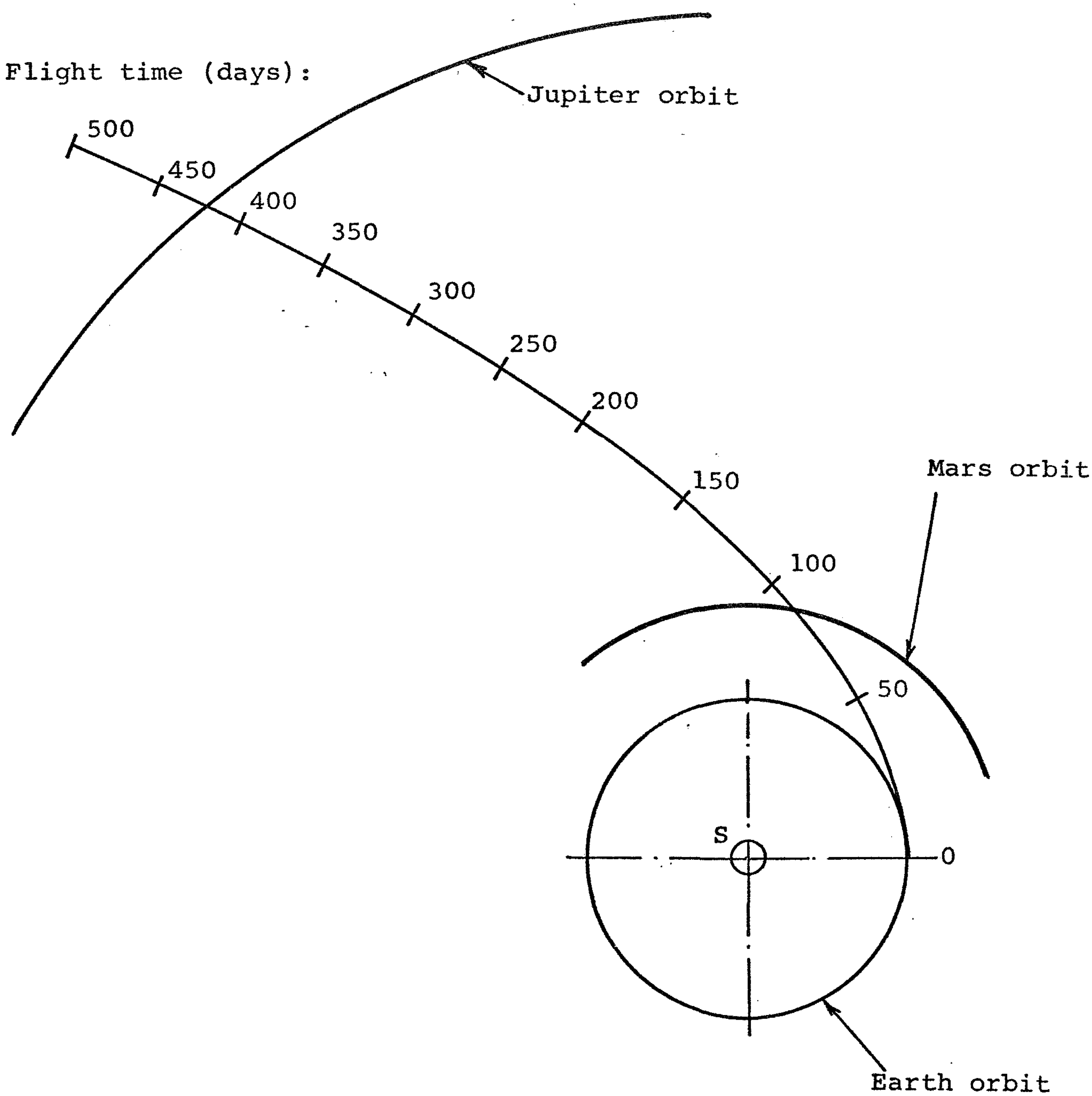

Figure 5. Sample Trajectory

($\lambda = 0.26$, $\beta = 0$, $q = 0.2$)

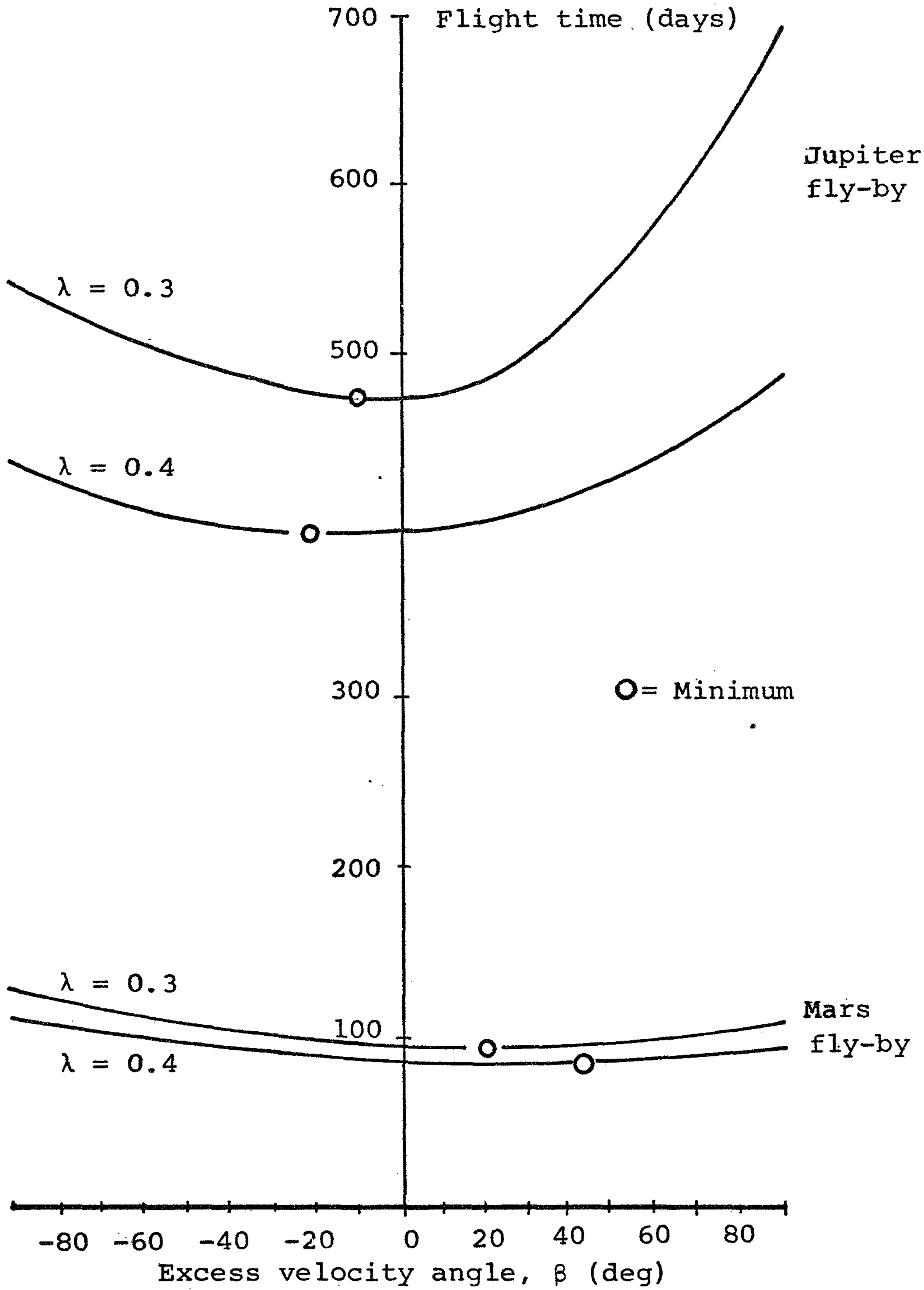

Figure 6. Effect of Excess Velocity Angle
(Launch excess velocity = 0.1)

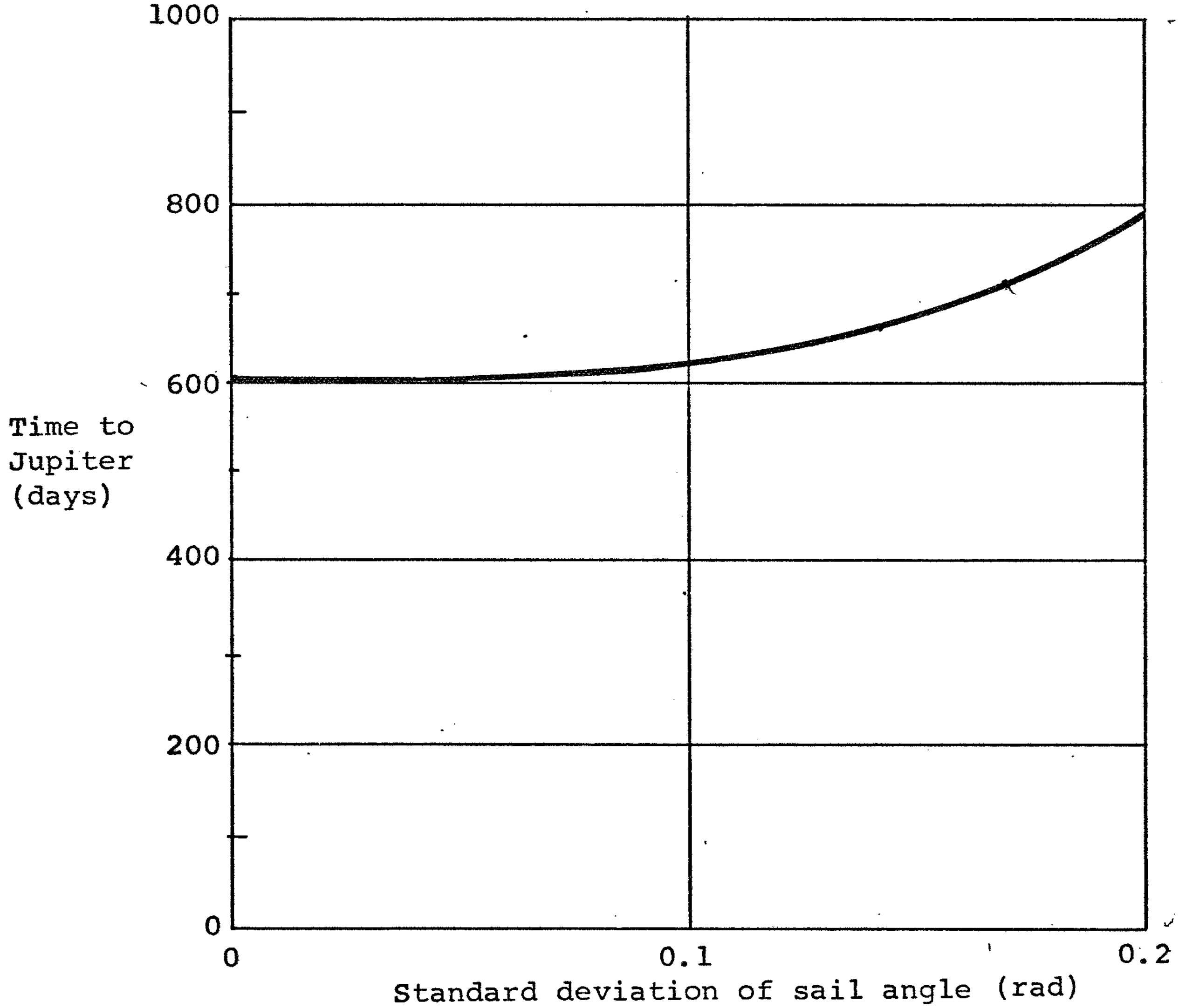

Figure 7. Effect of Random Errors
($\lambda = 0.15$; $q = 0.186$)

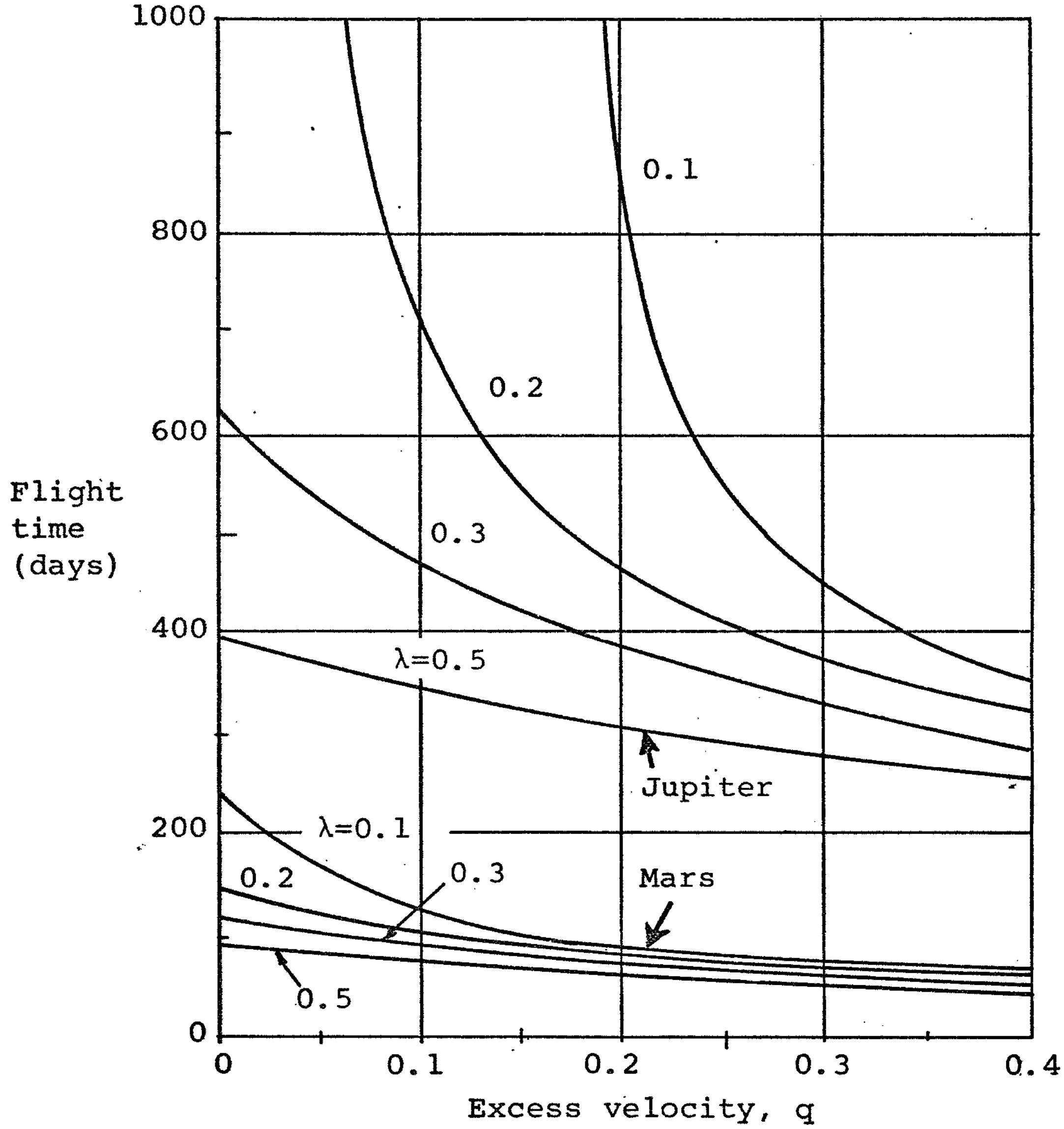

Figure 8. Basic Mission Results

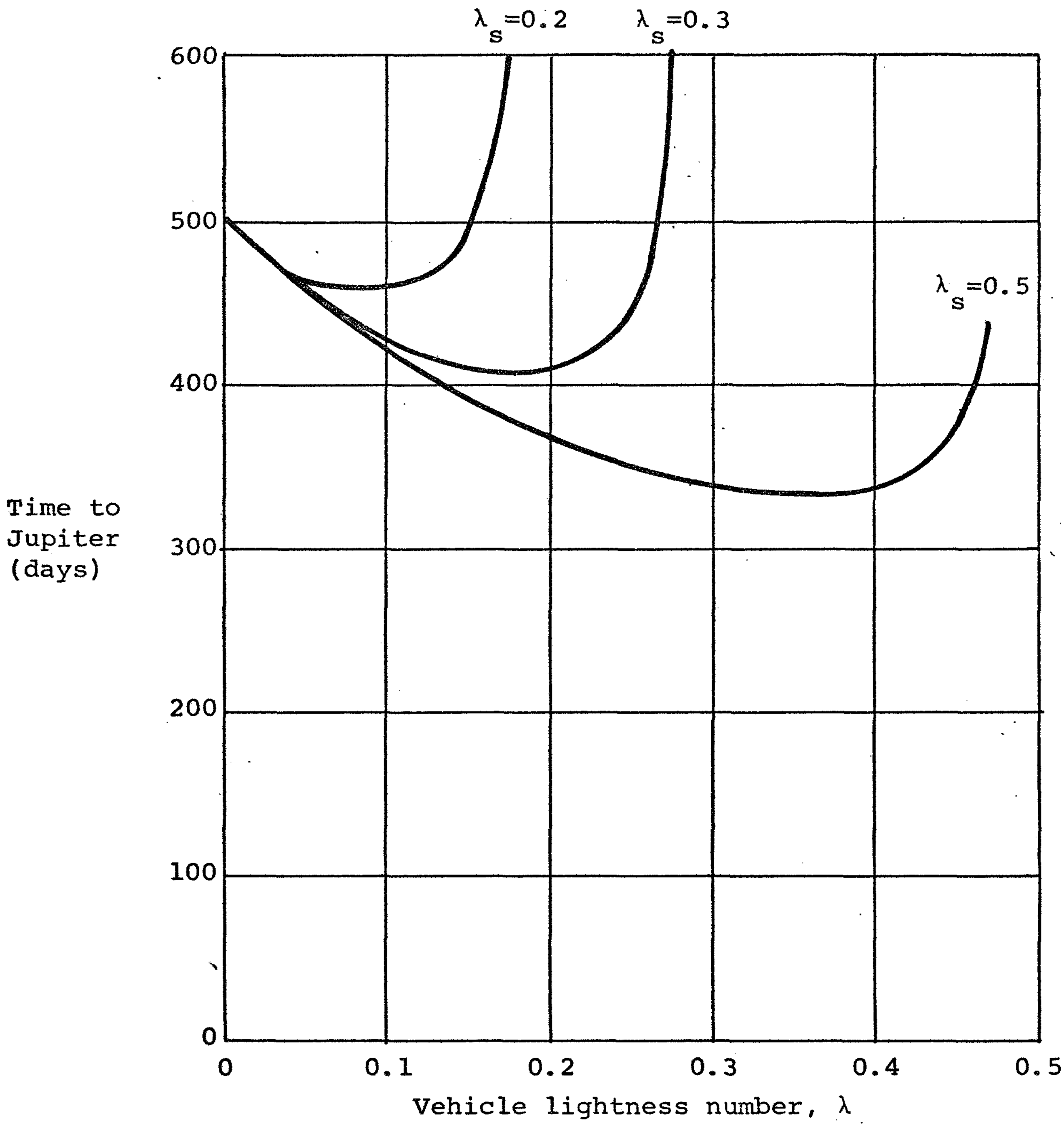

Figure 9. Variation in Flight Time with Vehicle Lightness Number for 227 kg Payload Mass and Fixed Sail Lightness Numbers (Titan IIIC/Burner II(1900) Launch Vehicle)

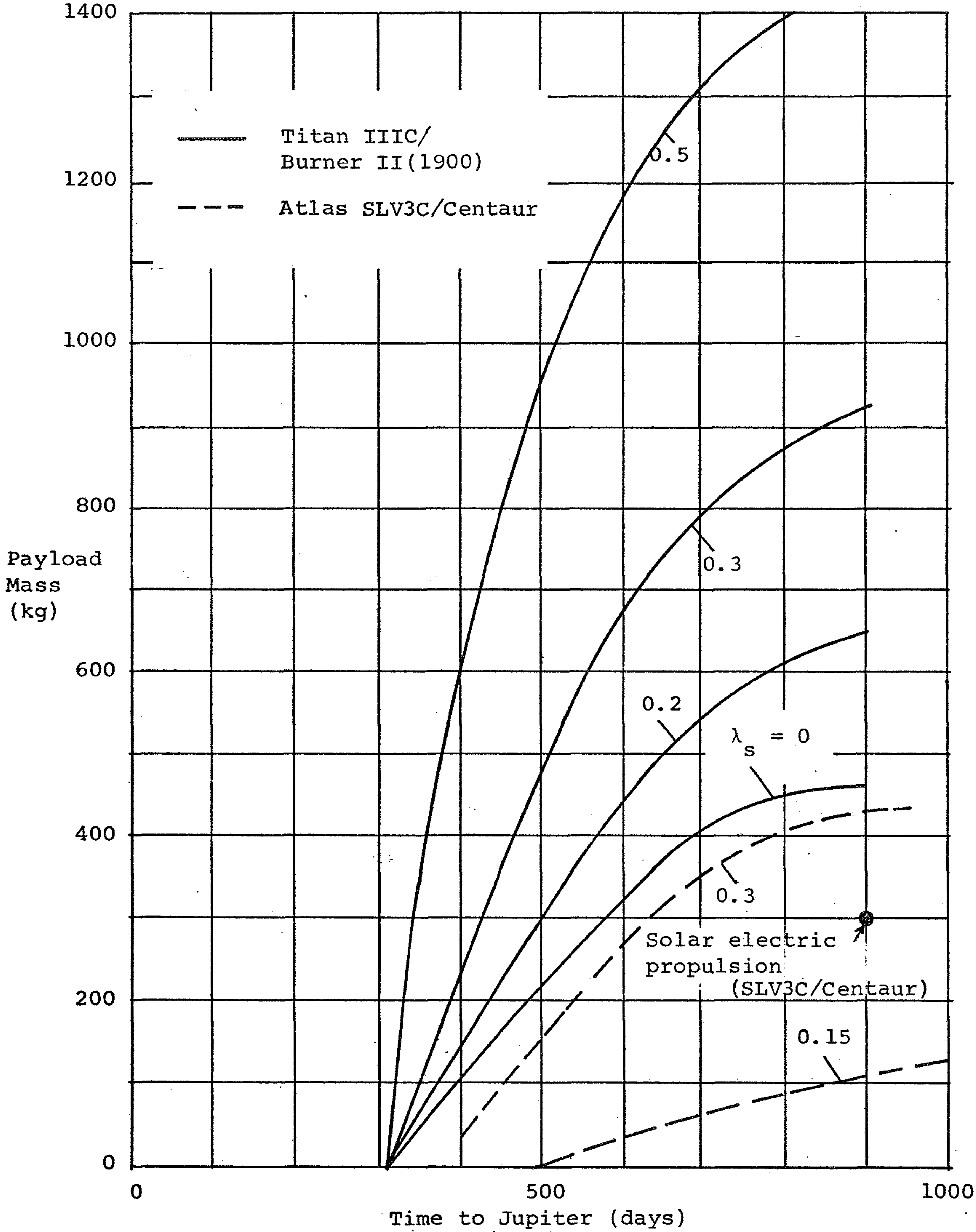

Figure 10. Jupiter Fly-by Heliogyro Mission Parameters